Supporting Information for

Tailoring sensing behavior of Cu@multi-wall carbon nanotubes/polydimethysiloxane strain sensor through surface Cu geometrical structure

Yao-Yao Bai[a], Bin Zhang[a,*], Zhe-Xuan Wang[a], Yujia Yang[a], Xu-Ping Wu[b,c], Guang-Ping Zhang[b,*]

[a] *Key Laboratory for Anisotropy and Texture of Materials, Ministry of Education, School of Materials Science and Engineering, Northeastern University, 3-11 Wenhua Road, Shenyang 110819, P. R. China*

[b] *Shenyang National Laboratory for Materials Science, Institute of Metal Research, Chinese Academy of Sciences, 72 Wenhua Road, Shenyang 110016, P. R. China*

[c] *School of Materials Science and Engineering, University of Science and Technology of China, Shenyang 110016, P. R. China*

**To whom correspondence should be addressed: zhangb@atm.neu.edu.cn*

gpzhang@imr.ac.cn

Three MWCNT films with different thicknesses were fabricated from three aqueous solutions with monodisperse MWCNTs via vacuum filtration. The compositions of the solutions are listed in Table S1. The solutions were prepared by adding MWCNTs and Triton X-100 in 1000 ml deionized water, and 10-minute sonicating (using Q700, sonicator Co. Ltd., USA) for 3 times under a power of 100 Watt. After each 10 minute sonication, the MWCNT solution was centrifuged for 30 min at a centrifuge speed of 6000 r/min. Then the film was prepared by filtering the monodisperse MWCNT solution through a 0.45 μm-thick cellulose filter using a vacuum-pump. At last, the as-filtered MWCNT films with different thicknesses were rinsed using deionized water to wash away the surfactant, Triton X-100, and dried at 80℃ for 4 hours.

Table S1. Compositions of MWCNT aqueous solutions and thicknesses of MWCNT films

Sample	MWCNTs (mg)	Triton X-100 (mL)	DI water (mL)	Thickness (μm)
1	500	5	1000	30
2	750	10	1000	60
3	1000	15	1000	80

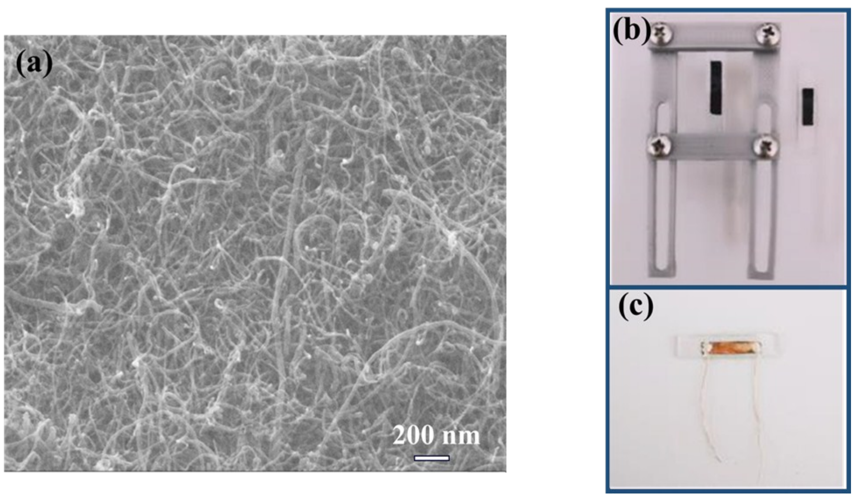

Fig. S1. (a) SEM image of as-prepared MWCNT film; Optical images of (b) stretched MP substrate and (c) as-fabricated Cu@MP strain sensor

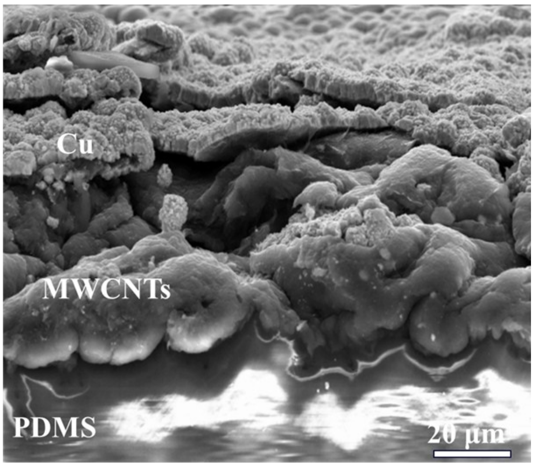

Fig. S2. Cross-sectional SEM image of Cu@MP hybrid film fabricated on 30% pre-strain substrate

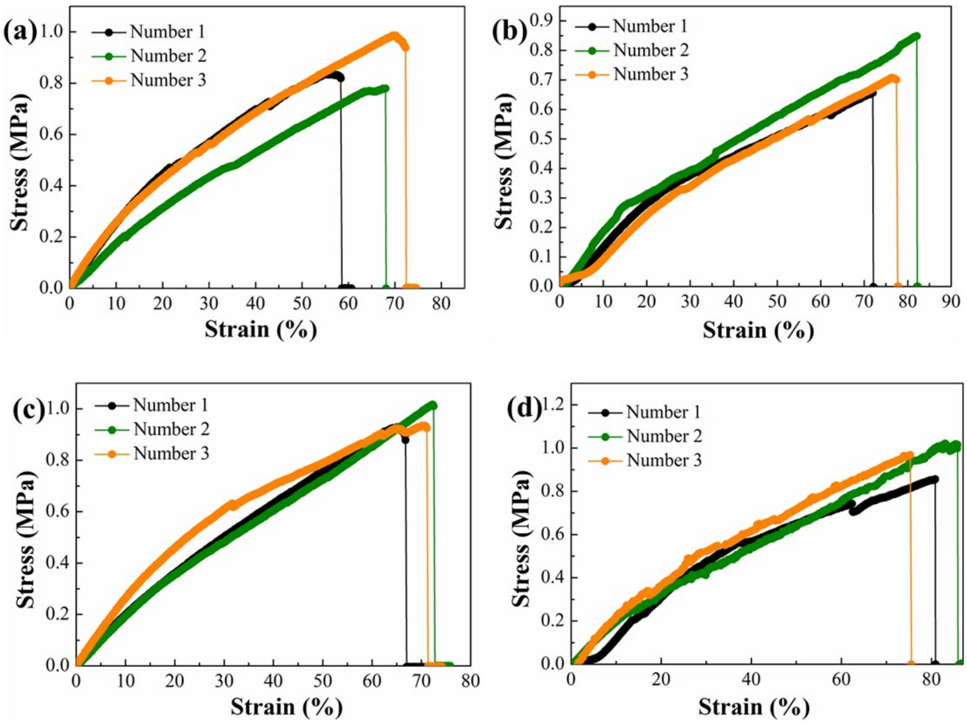

Fig. S3. Stress-strain curves of (a) MP, (b) 10%, (c) 20%, and (d) 30% pre-strain Cu@MP sensors, respectively

Table S2. Ultimate tensile stress and fracture strain of MP and pre-strain Cu@MP sensors

Sensors	Ultimate tensile stress (MPa)	fracture strain (%)
MP	0.84 ± 0.12	66 ± 8
10% pre-strain	0.74 ± 0.11	77 ± 5
20% pre-strain	0.94± 0.06	70 ± 4
30% pre-strain	0.94± 0.09	80 ± 5

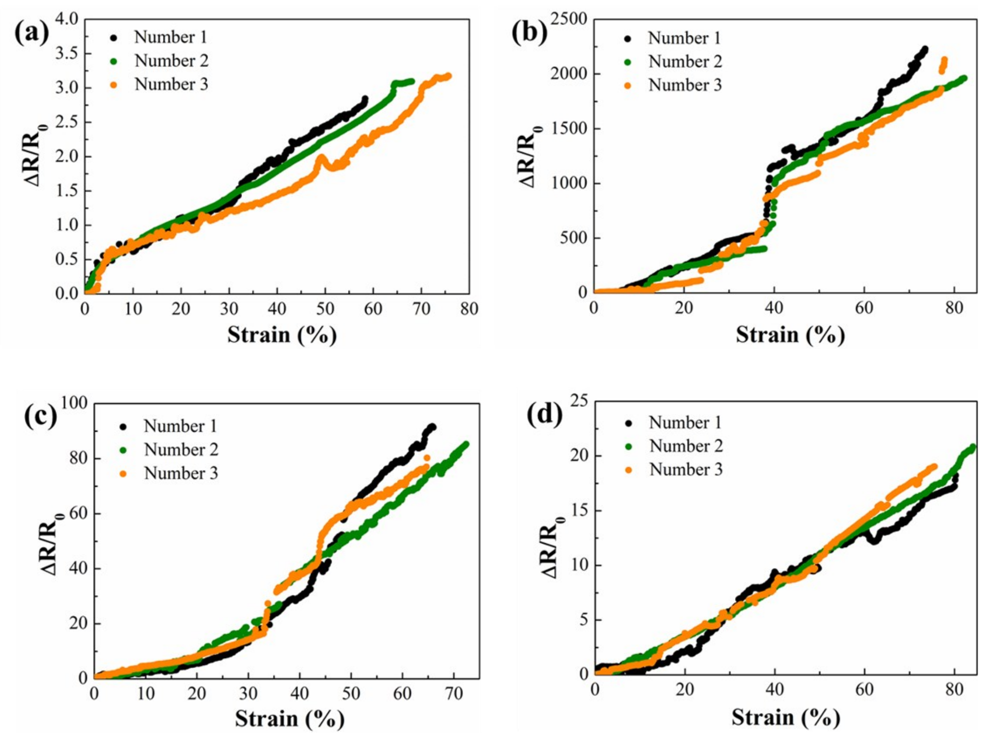

Fig. S4. Relative change in resistance as a function of strain for sensors of (a) MP, (b) 10%, (c) 20%, and (d) 30% pre-strain Cu@MP, respectively

Table S3. $\Delta R/R_0$ at different tensile strains for MP and corresponding pre-strain Cu@MP sensors

Tensile strain	MP sensors	10% pre-strain sensors	20% pre-strain sensors	30% pre-strain sensors
10%	0.67 ± 0.06	21.68 ± 4.66	3.65 ± 0.92	1.32 ± 0.72
30%	1.30 ± 0.11	401.19 ± 72.12	14.79 ± 1.17	5.66 ± 0.28
50%	2.19 ± 0.26	1277.20 ± 62.90	59.21 ± 7.46	10.96 ± 0.12
70%	2.98 ± 0.31	1816.92 ± 183	86.98 ± 4.32	16.20 ± 1.51

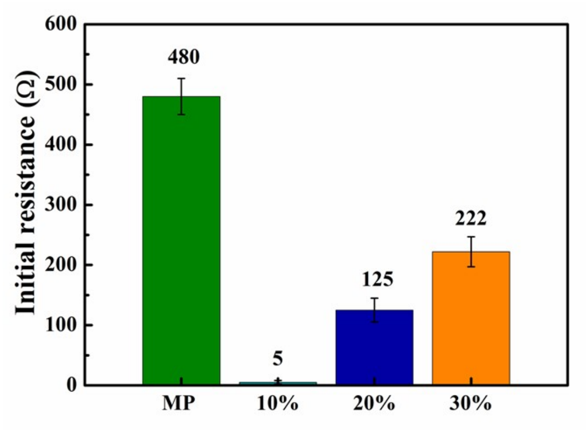

Fig. S5. Initial resistance of MP and corresponding pre-strain Cu@MP sensors

Element EDS mapping of C, Si and Cu which are the tracing elements of the MWCNTs, the PDMS and the Cu film of a sensor, respectively. An SEM image of a failured 10% pre-strain Cu@MP sensor with a large crack is shown in Fig. S6(a), and the corresponding element mapping are shown in Fig. S6(c), (d) and (e), respectively. The strong signals of all the three element mapping shown in Fig. S6(b) indicates the constitute of the sensor. The strong C and Si mapping (in red and blue, respectively) appeared at the large crack are correlated with MWCNTs and PDMS, respectively, proving the MWCNTs embedded in PDMS as aforementioned, and the continuous conductive network of MWCNTs still persisted when the Cu film fractured.

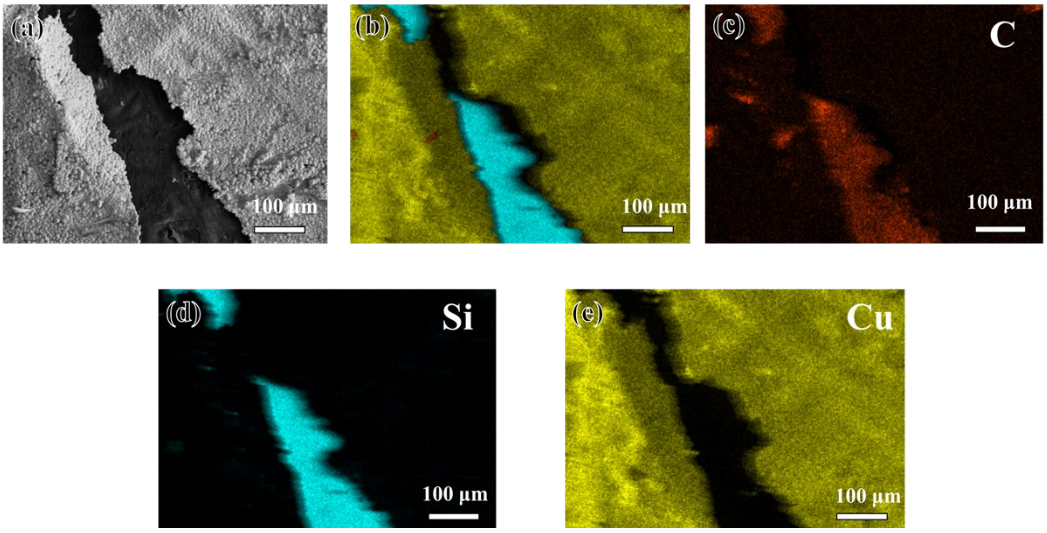

Fig. S6. (a) SEM image and (b-e) element mapping of 10% pre-strain Cu@MP sensor in Stage 3

Table S4. Parameter comparison of different strain sensors

Material	GF range	Strain range (%)	Ref.
Ti3C2Tx MXene/Carbon Nanotube	64.6-772.6	0-130	1
RGO/TPU	11-79	0-100	2
Graphene armour scales	200-1054	0-26	3
GNC/PDMS	87-1071	0-15	4
Ti3C2Tx MXene- Graphene	190.8-1148.2	0-74.1	5
Crack-based Ni@Graphene Wrapped Polyurethane Sponge	36.03-3360.	0-65	6
Aligned fiber based CPCs	50-593	0-150	7
RGO/PDMS	7-173	0-40	8
Wrinkled Platinum Sensor	0-42	0-185	9
Fish Scale-Like Graphene	16.2-150	0-82	10
10% pre-strain Cu@MP Sensor	**263-2387**	**0-82**	**Present work**

Reference

1. Y. Cai, J. Shen, G. Ge, Y. Zhang, W. Jin, W. Huang, J. Shao, J. Yang and X. Dong, *ACS Nano*, 2018, **12**, 56-62.
2. Y. Wang, J. Hao, Z. Huang, G. Zheng, K. Dai, C. Liu and C. Shen, *Carbon*, 2018, **126**, 360-371.
3. Y. F. Yang, L. Q. Tao, Y. Pang, H. Tian, Z. Y. Ju, X. M. Wu, Y. Yang and T. L. Ren, *Nanoscale*, 2018, **10**, 11524-11530.
4. P. Xue, C. Chen and D. Diao, *Carbon*, 2019, **147**, 227-235.
5. Y. Yang, Z. Cao, P. He, L. Shi, G. Ding, R. Wang and J. Sun, *Nano Energy*, 2019, **66**, 104134.
6. F. Han, J. Li, S. Zhao, Y. Zhang, W. Huang, G. Zhang, R. Sun and C.-P. Wong, *J. Mater. Chem. C*, 2017, **5**, 10167-10175.
7. G. Li, K. Dai, M. Ren, Y. Wang, G. Zheng, C. Liu and C. Shen, *Journal of Materials Chemistry C*, 2018, **6**, 6575-6583.
8. Y. J. Yun, J. Ju, J. H. Lee, S.-H. Moon, S.-J. Park, Y. H. Kim, W. G. Hong, D. H. Ha, H. Jang, G. H. Lee, H.-M. Chung, J. Choi, S. W. Nam, S.-H. Lee and Y. Jun, *Advanced Functional Materials*, 2017, **27**, 1701513.
9. J. D. Pegan, J. Zhang, M. Chu, T. Nguyen, S. J. Park, A. Paul, J. Kim, M. Bachman and M. Khine, *Nanoscale*, 2016, **8**, 17295-17303.
10. Q. Liu, J. Chen, Y. Li and G. Shi, *ACS Nano*, 2016, **10**, 7901-7906.